Med Chem Res
DOI 10.1007/s00044-013-0907-7

MEDICINAL CHEMISTRY RESEARCH

ORIGINAL RESEARCH

Synthesis, characterization, electrochemical behavior, and antimicrobial activities of aromatic/heteroaromatic sulfonylhydrazone derivatives

Ayla Balaban Gündüzalp · Ümmühan Özdemir Özmen · Bekir Sıtkı Çevrimli · Serhat Mamaş · Servet Çete

Received: 2 November 2013 / Accepted: 30 December 2013

Abstract The aromatic/heteroaromatic sulfonylhydrazone derivatives as indole-3-carboxaldehyde methanesulfonylhydrazone (**1**), indole-3-carboxaldehydeethanesulfonyl hydrazone (**2**), thiophene-2-carboxaldehydeethanesulfonylhydrazone (**3**), 2-hydroxybenzaldehydeethanesulfonyl hydrazone (**4**), 2-hydroxyacetophenoneethanesulfonylhydrazone (**5**) and 2-hydroxy-1-naphth aldehydeethane sulfonylhydrazone (**6**) were synthesized by the reaction of sulfonic acids with aromatic/heteroaromatic aldehydes and characterized by using elemental analysis, ^{1}H–^{13}C NMR, LC–MS and IR spectra. The electrochemical behavior of the sulfonylhydrazones in DMSO at glassy carbon electrode was investigated using cyclic voltammetry, controlled potential electrolysis and chronoamperometry techniques. The number of electrons transferred, diffusion coefficient and standard heterogeneous rate constants were determined using electrochemical methods. Antimicrobial activities of the compounds **1**–**6** were tested against some microorganisms. The biological activity screening showed that compound **6** exhibited better activity than the others. Structure–activity relationship analysis of the sulfonylhydrazone derivatives was performed to explain the trend of activity with molecular descriptors. The indicator descriptors for compound **6** having naphtyl ring are the most important descriptos that are sensitive both to the size and electrophility of the molecules.

A. B. Gündüzalp (✉) · Ü. Ö. Özmen · S. Mamaş · S. Çete
Department of Chemistry, Faculty of Arts and Science, Gazi University, Teknikokullar, Ankara, Turkey
e-mail: balaban@gazi.edu.tr

B. S. Çevrimli
Department of Chemistry, Atatürk Vocational School, Gazi University, Akyurt, Ankara, Turkey

Keywords Sulfonylhydrazones · Electrochemical behavior · Antimicrobial activity · Well diffusion method

Introduction

The sulfonamides (–SO_2NH–) are used widely as antibacterial agents because of their lower cost, lower toxicity and most activity against bacterial diseases (Özçelik *et al.*, 2004). Sulfo drugs are used as chemotherapeutic agents with large spectrum of activity and they are widely used today for various bacterial, protozoal and fungal infections (Alyar *et al.*, 2012a, b). Methane sulfonamide derivatives possess DNA-binding ability and show cytostatic effects which have usage in cancer chemotherapy. Having hydrophilic characters like sulfonyl group are considered as a suitable pharmacophoric equivalent for replacing active sites in drug design (Jensen *et al.*, 1990; Finlay *et al.*, 1990; Alyar *et al.*, 2011a, b). Sulfonylhydrazones derived from sulfonamides have pharmacological properties as antibacterial, antitumor, diuretic, antiviral, antinociceptive activity and enzyme inhibition especially to carbonic anhydrase species (Dodoff *et al.* 1999; Özdemir *et al.* 2010). Many of the physiologically active hydrazones have applications in the treatment of illness like tuberculosis, leprosy, and mental damage. For this reason, the electrochemical behavior of the hydrazones may be very helpful for their efficient uses. The enlightening of the electroreduction mechanism can serve as models for the biological pathway of the hydrazones, because their activity depends on reductive processes in the body. The chemical and biological activities of the hydrazones vary in different media. Accordingly, the knowledge of the electrochemical reduction of these compounds is useful to understand their

Published online: 17 January 2014

mechanism in chemical and biological processes (Demirel Özel *et al.*, 2009). Due to the widespread usage of the hydrazones in drug industry, the redox properties of these compounds are thought to be useful to understand the metabolic fate of the drug-containing hydrazones or pharmacological activities (Baymak *et al.*, 2003; Aleksic *et al.*, 2004).

Electrochemical reduction mechanism of sulfonylhydrazones was also proposed that hydrazones have electrochemical reduction (EC) mechanism corresponding to semireversible two electron transfer steps and that a radical anion formed in the first step followed rapid proton abstraction and a second electron transfer. Electrochemical reduction (EC) mechanism contributes to the suggestion of the biochemical behavior of the hydrozones (Demirel Özel *et al.*, 2009).

In previous studies, we reported the antibacterial and cytotoxic effect of methanesulfonic acid hydrazide (**msh**: $CH_3SO_2NHNH_2$) and its hydrazone derivatives (Dodoff *et al.*, 1999) as well as their transition metal carbonyl complexes (Özdemir *et al.*, 2003; Sert *et al.*, 2004; Özdemir *et al*., 2004; Özdemir *et al*., 2006). In this article, six aromatic/heteroaromatic sulfonylhydrazone derivatives; indole-3-carboxaldehydemethanesulfonylhydrazone (**1**), indole-3-carboxaldehydeethanesulfonylhydrazone (**2**), thiophene-2-carboxaldehydeethanesulfonylhydrazone (**3**), 2-hydroxy benzaldehydeethanesulfonyl hydrazone(**4**), 2-hydroxyacetophenoneethanesulfonylhydrazone (**5**), and 2-hydroxy-1-naphthaldehydeethane sulfonylhydrazone (**6**) have been synthesized by the reaction of methane sulfonic acid hydrazide (**msh**: $CH_3SO_2NHNH_2$) and ethane sulfonic acid hydrazide (**esh**: $CH_3CH_2SO_2NHNH_2$) with aromatic/heteroaromatic aldehydes and characterized using elemental analysis, ^1H–^{13}C NMR, LC–MS, and IR spectra.

The electrochemical behaviors of aromatic/heteroaromatic sulfonylhydrazones were evaluated by cyclic voltammetry (CV), controlled potential electrolysis, and chronoamperometry (CA) techniques in the presence of 0.10 M tetrabutylammonium tetrafluoroborate (TBATFB) in dimethylsulfoxide (DMSO) at glassy carbon electrode. The number of electrons transferred (n), and diffusion coefficients (D) were determined using an ultramicro electrode (UME). The standard heterogeneous rate constants (k_s) were calculated using Klingler–Kochi technique. Electrochemical reduction mechanism of these aromatic/heteroaromatic sulfonylhydrazones was also proposed that sulfonylhydrazones follow electrochemical reduction (EC) mechanism which follows semireversible electron transfer steps.

Antimicrobial activities of the compounds **1**–**6** have been tested against *Pseudomonas aeroginosa* ATCC 29212, *Bacillus cereus* RSKK 863, *Micrococcus luteus* NRLL B-4375, *Staphylococcus aureus* ATCC 259231, *Yersinia enterocolitica* ATCC 1501 and Yeast Cell: *Candida albicans* ATCC 10239. The activities were determined by well-diffusion method and results were exhibited as inhibition zone diameter (mm) (Alyar *et al.*, 2011a, b). The geometry optimization was performed on B3LYP/6-311G(*d*,*p*) methods with GAUSSIAN 03 software. The molecular descriptors such as log*P*, dipole moment (DM), surface area (SA), volume(V), refractivity (R), mass (M), hydration enthalpy(ΔH_{hyd}), binding energy (ΔE_b), heat of formation (ΔH_f), and HOMO and LUMO energies were determined with Hyperchem 8 PM3-based QSAR models, respectively. Reduction potentials of C=N, OH and SO_2 groups were evaluated with molecular descriptors. Structure–activity relationship (SAR) analysis of the sulfonylhydrazone derivatives was performed to explain the effect of the molecular descriptors on biological activity (Özbek *et al.*, 2009).

Experimental section

Physical measurements

Elemental analysis was performed according to standard microanalytical procedures using LECO CHNS-932 model (TÜBİTAK Laboratories, Ankara). ^1H–^{13}C NMR spectra of dimethylsulfoxide-d_6 (DMSO-d_6) solutions of the compounds were registered on a Bruker WM-400 spectrometer (400 MHz) using tetramethylsilane as internal standard. D_2O-exchange was applied to confirm the assignment of the NH- and OH-signals (compounds **4–6**). The infrared spectra of the compounds as KBr-disks were recorded in the range of 4000–400 cm^{-1} with a Mattson 1000 FT-IR spectrometer. Melting points of sulfonamide derivatives were determined with a Gallenkamp melting point apparatus. The solvents used were purified and distilled according to routine procedures. 2-Hydroxy-1-naphthaldehyde and indole-3-carboxaldehyde were recrystallized from aqueous ethanol. Methanesulfonyl chloride, ethanesulfonyl chloride, hydrazine hydrate, thiophene-2-carboxaldehyde, indole-3-carboxaldehyde, 2-hydroxybenz aldehyde, 2-hydroxyacetophenone, and 2-hydroxy-1-naphthaldehyde were commercial products (purum).

Synthesis of the aromatic/heteroaromatic sulfonylhydrazone derivatives

The procedure of preparation of sulfonylhydrazone derivatives **1–6** is similar to that applied by us (Dodoff *et al.*, 1999; Özdemir Özmen and Olgun, 2008). Thus, solution of 1.10 g (10 mmol) methanesulfonic acid hydrazide or ethanesulfonic acid hydrazide in 5 ml of water was mixed with hot solution of 12 mmol of the corresponding

carbonyl compound (thiophene-2-carboxyaldehyde, indole-3-carboxaldehyde, 2-hydroxybenzaldehyde, 2-hydroxyacetophenone, and 2-hydroxy-1-naphthaldehyde, respectively) in 10 ml of ethanol and stirred for 1 h. Upon cooling, the obtained crystalline precipitates were filtered, washed with ethanol-ether, recrystallized from water and dried in vacuo over P_2O_5. They are colorless and light yellow crystalline solids, stable at normal conditions and soluble in methanol, ethanol, acetonitrile, dimethylformamide, DMSO and poorly soluble in benzene, water.

Indole-3-carboxaldehydemethanesulfonylhydrazone (1)

The general synthetic method described above afforded a yellowish needles solid from methanesulfonic acid hydrazide (10 mmol) and indole-3-carboxaldehyde (12 mmol). The results were as follows: yield 60 %; m.p. 144–145 °C; IR (KBr) = 3190 (s, νNH), 1628 (m, νC=N), 1317 (s, $\nu_{as}(SO_2)$, 1157 (s, $\nu_{sym}SO_2$), 650 (w, δNH), 520 (m, δSO_2); ^{1}H NMR (400 MHz, DMSO-d_6); δ = 12.99 (s, 1H, $NH_{(ring)}$), 10.01 (s, 1H, NH), 8.36 (s, 1H, N=CH–10), 7.94 (s, 1H, H-2), 7.79 (d, 1H, H-5), 7.24 (d, 1H, H-8), 7.08 (t, 1H, H-7), 7.06 (t, 1H, H-6), 3.08 (s, 3H, CH_3-11); ^{13}C NMR (100.62 MHz, DMSO-d_6): δ = 159.6 (HC=N, C-10), 138.7 (CH, C-2), 133.4 (C, C-9), 132.6 (C, C-4), 120.5 (CH, C-7), 119.2 (CH, C-6), 119.1 (CH, C-5), 117.7 (C, C-3), 110.9 (CH, C-8), 46.7 (CH_3, C-11); EIMS *m/z* 238.1 (36) $[M]^+$, 107.1 (87) $[CH_3N_2SO_2]^+$; Anal. Calcd. for: $C_{10}H_{11}N_3SO_2$ (237.1433 g/mol): calcd. C, 50.634; H, 4.644; N, 17.723; S, 13.498; found: C, 51.019; H, 4.864; N, 17.937; S, 13.822.

Indole-3-carboxaldehydeethanesulfonylhydrazone (2)

The general synthetic method described above afforded a yellowish solid from ethanesulfonic acid hydrazide (10 mmol) and indole-3-carboxaldehyde (12 mmol). The results were as follows: yield: 55–65 %; m.p. 158–160 °C; IR (KBr) = 3191 (s, νNH), 1627 (m, νC=N), 1320 (s, $\nu_{as}(SO_2)$, 1157 (s, $\nu_{sym}SO_2$), 707(w, δNH), 527 (m, δSO_2); ^{1}H NMR (400 MHz, DMSO-d_6); δ = 12.97 (s, 1H, $NH_{(ring)}$), 11.22 (s, 1H, NH), 8.08 (s, 1H, N=CH-10), 7.62 (s, 1H, H-2), 7.49 (d, 1H, H-5), 7.23 (d, 1H, H-8), 6.96 (t, 1H, H-7), 6.94 (t, 1H, H-6), 3.13 (s, 2H, SO_2CH_2-11), 1.13 (s, 3H, CH_3-12); ^{13}C NMR (100.62 Mz, DMSO-d_6): δ = 159.8 (HC=N, C-10), 139.6 (CH, C-2), 133.6 (C, C-9), 132.9 (C, C-4), 120.2 (CH, C-7), 119.8 (CH, C-6), 119.6 (CH, C-5), 118.1 (C, C-3), 111.3 (CH, C-8), 46.9 (SO_2CH_2, C-11), 9.1 (CH_3, C-12); EIMS *m/z* 252.0 (33) $[M]^+$; 93.0 (100) $[C_2H_5SO_2]^+$; Anal. Calcd. for: $C_{11}H_{13}N_3SO_2$ (251.1243 g/mol): calcd. C, 52.566; H, 5.215; N, 16.723; S 12.763 found: C, 52.314; H, 5.390; N, 16.926; S, 12.473.

Thiophene-2-carboxaldehydeethanesulfonylhydrazone (3)

The general synthetic method described above afforded a light yellow crystalline solid from mmol ethanesulfonic acid hydrazide (10 mmol) and thiophene-2-carboxaldehyde (12 mmol). The results were as follows: yield: 70 %; m.p. 110–112 °C; IR (KBr) = 3198 (s, νNH), 1611 (m, νC=N), 1329 (s, $\nu_{as}(SO_2)$, 1157 (s, $\nu_{sym}SO_2$), 709 (w, δNH), 515 (m, δSO_2); ^{1}H NMR (400 MHz, DMSO-d_6); δ = 11.15 (s, 1H, NH), 8.02 (s, 1H, N=CH-6), 7.47 (d, 1H, H-5), 7.29 (d, 1H, H-3), 6.97 (t, 1H, H-4), 3.00 (s, 2H, SO_2CH_2-7), 1.07 (s, 3H, CH_3-8); ^{13}C NMR (100.62 MHz, DMSO-d_6); δ = 142.8 (N=CH, C-6), 139.0 (C, C-2), 131.5 (CH, C-3), 129.5 (CH, C-5), 128.5 (CH, C-4), 39.2 (SO_2CH_2, C-7), 8.6 (CH_3, C-8); EIMS *m/z* 217.1 (45) $[M]^+$; 121.8 (34) $[C_2H_5N_2SO_2]^+$; Anal. Calcd. for: $C_7H_{10}N_2S_2O_2$ (218.2457 g/mol): calcd. C, 38.524; H, 4.623; N, 12.833; S, 31.394; found: C, 38.075; H, 4.479; N, 12.875; S, 31.162.

2-Hydroxybenzaldehydeethanesulfonylhydrazone (4)

The general synthetic method described above afforded a colorless solid from ethanesulfonic acid hydrazide (10 mmol) and 2-hydroxybenzaldehyde (12 mmol). The results were as follows: yield: 60 %; m.p. 133–134 °C; IR (KBr) = 3188 (s, νNH), 1625 (m, νC=N), 1320 (s, $\nu_{as}(SO_2)$, 1268 (s, νCO), 1142 (s, $\nu_{sym}SO_2$) 643 (s, δNH), 528 (m, δSO_2); ^{1}H NMR (400 MHz, DMSO-d_6); δ = 11.35 (s, 1H, OH), 10.23 (s, 1H, NH), 8.27 (s, 1H, N=CH-7), 7.56 (d, 1H, H-6), 7.49 (t, 1H, H-4), 6.92 (t, 1H, H-5), 6.88 (d, 1H, H-3), 3.22 (s, 2H, SO_2 CH_{2-8}), 1.22 (s, 3H, CH_3-9); ^{13}C-NMR (100.62 MHz, DMSO-d_6): δ = 154.9 (CO, C-2), 149.7 (N=CH, C-7), 131.9 (C, C-1), 128.9 (CH, C-6), 120.2 (CH, C-5), 119.1 (CH, C-4), 117.3 (CH, C-3), 45.1 (SO_2CH_2, C-8), 8.0 (CH_3, C-9); EIMS *m/z* 229.0 (76) $[M]^+$; 121.8 (34) $[C_2H_5N_2SO_2]^+$; Anal. Calcd. for: $C_9H_{12}N_2SO_3$ (228.1396 g/mol): calcd. C, 47.362; H, 5.263; N, 12.278; S, 14.030; found: C, 47.411; H, 5.453; N, 12.152; S, 13.943.

2-Hydroxyacetophenoneethanesulfonyl-hydrazone (5)

The general synthetic method described above afforded a light yellow solid from ethanesulfonic acid hydrazide (10 mmol) and 2-hydroxyacetophenone (12 mmol). The results were as follows: yield: 55 %, m.p. 142–143 °C; IR (KBr) = 3206 (s, νNH), 1642 (m, νC=N), 1339 (s, $\nu_{as}(SO_2)$, 1260 (s, νCO), 1160 (s, $\nu_{sym}SO_2$), 650 (w, δNH), 525 (m, δSO_2); ^{1}H NMR (400 MHz, DMSO-d_6); δ = 11.71 (s, 1H, OH), 10.60 (s, 1H, NH), 7.54 (d, 1H, H-6), 7.47 (t, 1H, H-4), 6.92 (t, 1H, H-5), 6.89 (d, 1H, H-3), 3.24 (s, 2H, SO_2 CH_2-8), 2.32 (s, 3H, N=CCH_3-7a), 1.27

(s, 3H, CH_3-9); ^{13}C NMR (100.62 MHz, DMSO-d_6): δ = 158.7 (CO, C-2), 157.9 (N=CH, C-7), 131.9 (C, C-1), 129.7 (CH, C-6), 121.0 (CH, C-5), 119.7 (CH, C-4), 118.1 (CH, C-3), 45.6 (SO_2CH_2, C-8), 15.0 (N=CCH_3-7a), 8.2 (CH_3, C-9); EIMS *m/z* 243.0 (100) $[M]^+$; Anal. Calcd. for: $C_{10}H_{14}N_2SO_3$ (242.1267 g/mol): calcd. C, 49.583; H, 5.777; N, 11.571; S, 13.221; found: C, 49.413; H, 5.558; N, 11.907; S, 12.964.

2-Hydroxy-1-naphthaldehydeethanesulfonylhydrazone (6)

The general synthetic method described above afforded a colorless solid from ethanesulfonic acid hydrazide (10 mmol) and 2-hydroxy-1-naphthaldehyde (12 mmol). The results were as follows: yield: 55 %, m.p. 185–186 °C; IR (KBr) = 3182 (s, νNH), 1625 (m, νC=N), 1329 (s, $\nu_{as}(SO_2)$), 1241 (s, νCO), 1151 (s, $\nu_{sym}SO_2$), 673 (w, δNH), 537 (m, δSO_2); ^1H NMR (400 MHz, DMSO-d_6); δ = 11.18 (s, 1H, OH), 11.15 (s, 1H, NH), 8.81 (s, 1H, N=CH-11), 8.39 (s, 1H, H-10), 7.49 (d, 1H, H-5), 7.43 (t, 1H, H-6), 7.37 (d, 1H, H-8), 7.29 (t, 1H, H-7), 7.26 (s, 1H, H-3), 3.15 (s, 2H, SO_2CH_2-12), 1.15 (s, 3H, CH_3-13); ^{13}C NMR (100.62 Mz, DMSO): δ = 159.4 (CO, C-2), 138.6 (N=CH, C-11), 134.3 (C, C-4), 130.0 (CH, C-10), 128.7 (CH, C-8), 128.2 (CH, C-6), 127.1 (CH, C-5), 123.8 (CH, C-7), 118.4 (C, C-9), 118.0 (CH, C-3), 110.8 (C, C-1), 46.5 (SO_2CH_2, C-12), 8.6 (CH_3, C-13); EIMS *m/z* 276.9 (17) $[M]^+$; 93.1 (100) $[C_2H_5SO_2]^+$; Anal. Calcd. for: $C_{13}H_{14}N_2SO_3$ (278.3257 g/mol): calcd. C, 56.103; H, 5.033; N, 10.074; S, 11.507; found: C, 55.855; H, 4.950; N, 10.023; S, 11.388. The structure of the compounds is exhibited in Fig. 1.

Preparation of microbial cultures

Microorganisms were provided from the culture collection of the Biotechnology Laboratory of the Science and Art Faculty of Gazi University, Turkey. *Pseudomonas aeroginosa* ATCC 29212, *Bacillus cereus* RSKK 863, *Micrococcus luteus* NRLL B-4375, *Staphylococcus aureus* ATCC 259231, *Yersinia enterocolitica* ATCC 1501, and *Yeast Cell: Candida albicans* ATCC 10239 were used as the test organisms in this study. *Candida albicans* was inoculated into YPD Broth (Difco) and incubated at 30 °C for 48 h. Bacterial strains were inoculated into Nutrient Broth (Difco) and incubated at 30 ± 0.1 °C for 24 h. In order to test the antimicrobial effects of sulfonyl hydrazone derivatives, 15 mL of Mueller–Hinton agar (Merck) for bacteria, and YPD Agar (Merck) were placed in petri dishes which were then inoculated with strains of bacteria by taking 100 µL from cell culture media. In order to test the antimicrobial effects, sulfonyl hydrazone derivatives and 15 mL of YPD Agar (Merck) were placed in petri dishes which were then inoculate temperature for a while, and then holes were made on top with a sterile stick. It was left to solidify at room entities stated above were then added to these holes. Petri dishes were left at 4 °C for 2 h. Then, bacterial cultures were incubated at 34 ± 0.1 °C for 24 h, and yeast cultures were incubated at 30 ± 0.1 °C for 72 h. And the end of incubation time, the inhibition zones on the bacterial and yeast nutrient media were measured as diameter zone, mm (Özdemir *et al*., 2009; Özdemir *et al*., 2013). The control samples were only absorbed in DMSO. The antimicrobial activity results are the average data of three experiments.

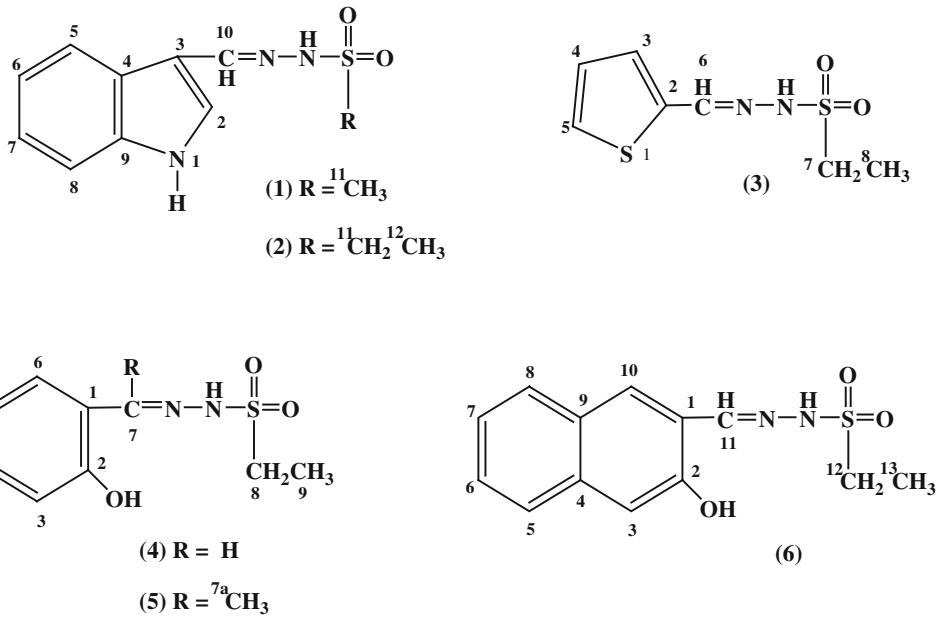

Fig. 1 The structure of the aromatic/heteroaromatic sulfonylhydrazones (**1**–**6**)

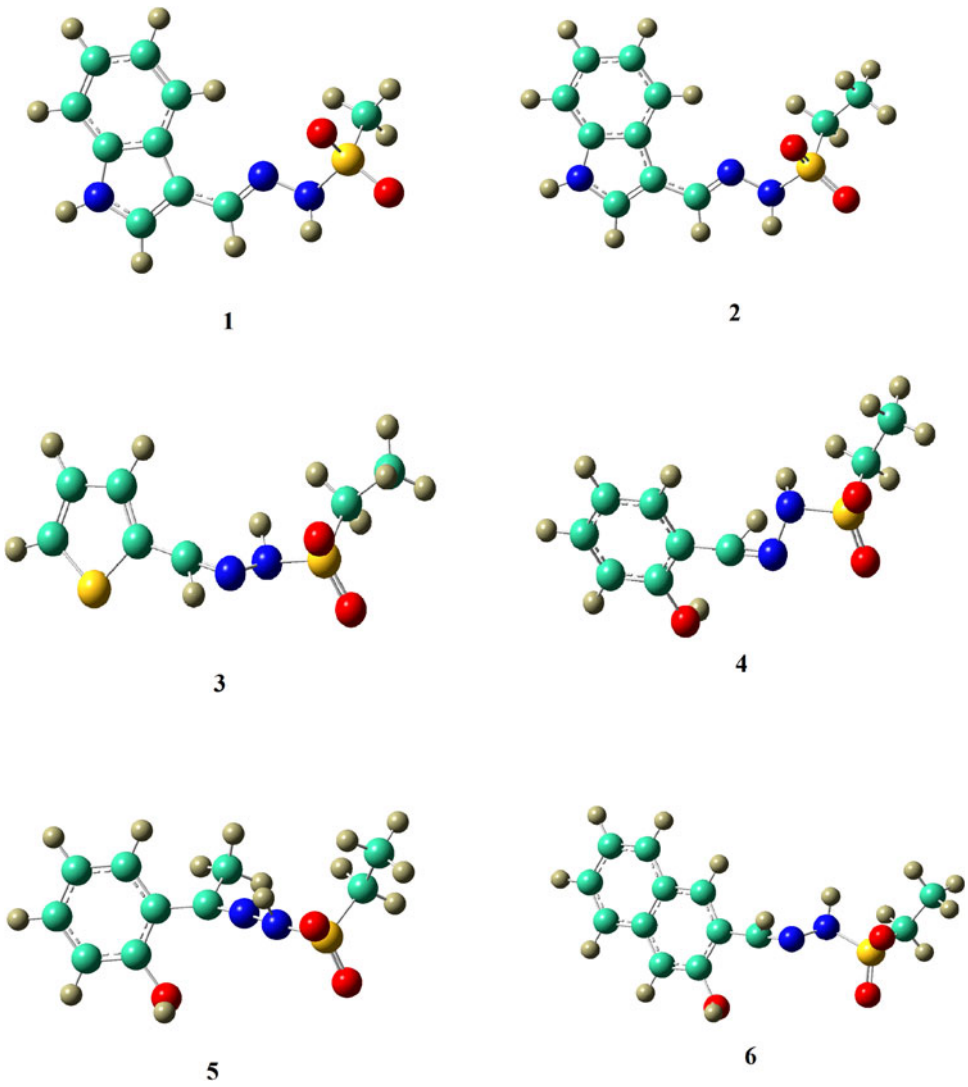

Fig. 2 Optimized geometries (DFT/B3LYP/6-311G(*d*,*p*)) of conformations

Electrochemical studies

Voltametric measurements were carried out with IVIUM Stat Electrochemical Analyzer. Glassy carbon electrode (BAS MF-2012) and 11 μm-ultramicro carbon electrode (BAS MF-2007) were used as a working electrode. The electrodes were polished with 1, 0.3 and 0.05 μm alümina slurries made from dry Buehler alumina and ultra pure water (18 MΩ cm) on polishing microcloth before each use. A platinum wire was used as the auxiliary electrode (BAS MW-1032). The reference electrode was a silver wire in contact with 0.01 M $AgNO_3$ in dimethylsulfoxide (BAS MF-2052). All solutions were deaerated for 10 min. with pure nitrogen. All the measurements were taken at room temperature, 21 ± 1 °C. For each measurements, the background currents were automatically subtracted from obtained currents.

The number of electrons transferred and diffusion coefficients were determined using ultramicro electrode CV technique of Baranski (Nora and de Souza 2005). And also, the heterogeneous rate constants were calculated according to Klingler–Kochi method (Alyar and Karacan 2009).

Computational section

The DFT calculations were carried out using Becke's three-parameter hybrid functional (B3LYP) method (Karacan *et al.*, 2012; Özbek *et al.*, 2012; Alyar *et al.*, 2012a, b). The geometry optimizations were performed for the ground states of these compounds, and these ground states were assumed to be a singlet state (Bajaj *et al.*, 2005). All the above-mentioned calculations for geometry optimization (Fig. 2) and HOMO and LUMO shapes (Fig. 3) were

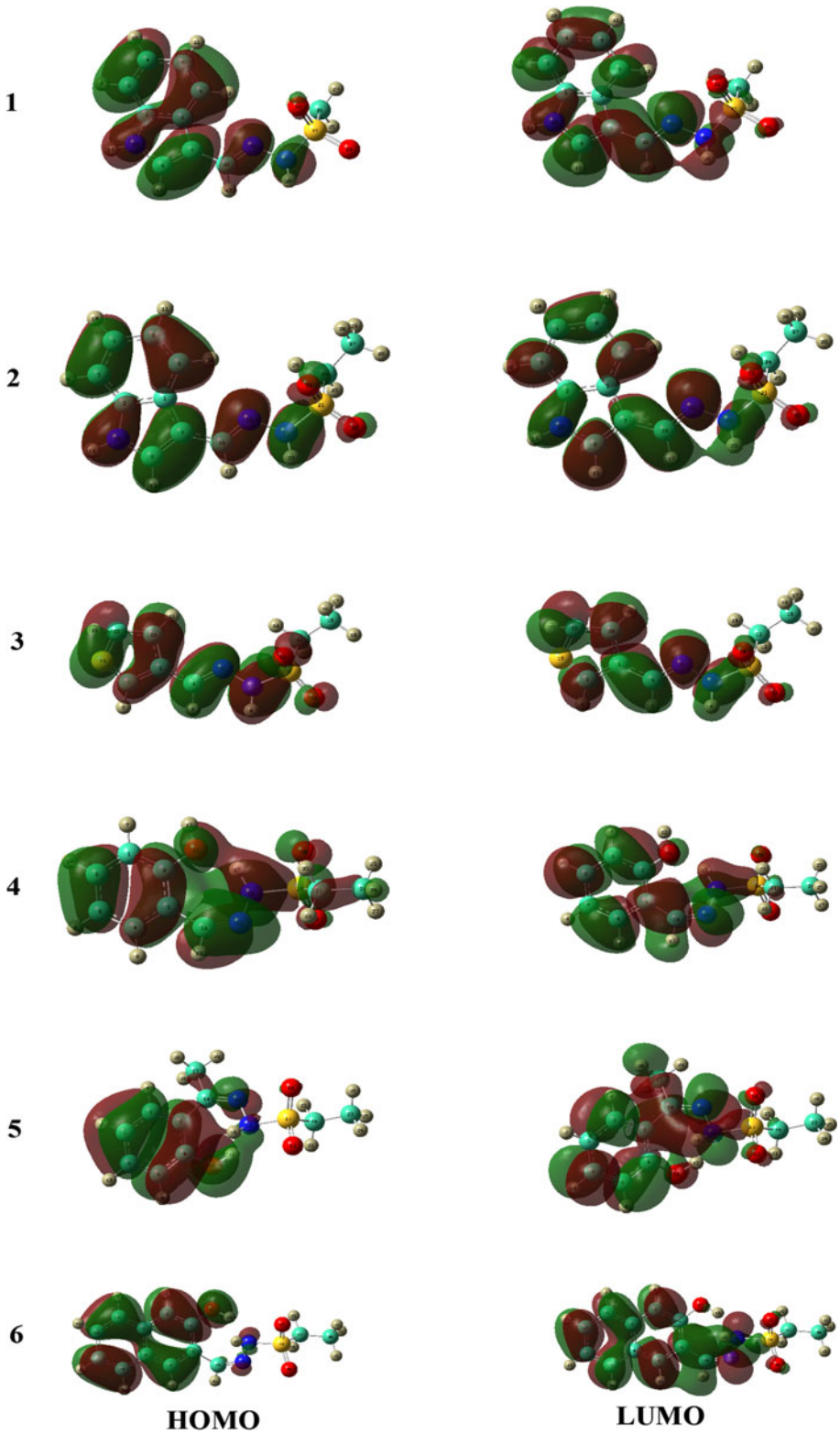

Fig. 3 HOMO and LUMO shapes along with the electrostatic potential maps of the sulfonylhydrazones

carried out by GAUSSIAN 03 quantum chemistry program-package (Rohrbaugh and Jurs 1987). The molecular descriptors such as logP, dipole moment (DM), surface area (SA), volume(V), refractivity (R), mass (M), hydration enthalpy (ΔH_{hyd}), binding energy (ΔE_b), heat of formation (ΔH_f), and HOMO and LUMO energies were determined by means of Hyperchem 8, PM3-based QSAR models to determine the structure–activity relation.

The octanol–water partition coefficient (log*P*) has been considered as descriptors of the hydrophobic effect. The dipole moment can be used to qualitatively analyze the trend in the hydrophobic values (log*P*). Surface area, volume, refractivity, and mass parameters depend on the size of molecules and also, binding energy, heat of formation, and hydration enthalpy are the thermodynamic parameters. The frontier molecular orbitals, in particular, the highest occupied molecular orbital (HOMO) and the lowest unoccupied molecular orbital (LUMO) are very important because they are related not only to the spectral properties, but also to the activity of the compounds.

Results and discussion

The structure of the aromatic/heteroaromatic sulfonylhydrazone derivatives (Fig. 1) named as indole-3-carboxaldehydemethane sulfonylhydrazone (**1**), indole-3-carboxaldehydeethanesulfonyl hydrazone (**2**), thiophene-2-carboxaldehydeethanesulfonylhydrazone (**3**), 2-hydroxybenzaldehyde ethanesulfonylhydrazone (**4**), 2-hydroxyacetophenoneethanesulfonylhydrazone (**5**) and 2-hydroxy-1-naphthaldehydeethanesulfonylhydrazone (**6**) have been characterized using elemental analysis, ^{1}H–^{13}C NMR, LC–MS and IR spectra. The electrochemical behavior and antimicrobial activities of the sulfonylhydrazones were investigated as mentioned below and correlated with functional groups in the structure (SAR's).

NMR spectra

The comparison of the spectra of the aldehyde (in compound **1–4**, **6**) and ketone (in compound **5**) derivatives facilitate the distinguishing of the signals of the methyl protons from the $CH_3C{=}N$ (Özdemir *et al.*, 2006), CH_3SO_2 fragments and the HC=N protons (Dodoff *et al.*, 1999). For salicylaldimines and related compounds which regarded as potentially tautomeric systems, phenol–imine and quinoid form being possible much number of sulfonylhydrazones, it has been shown that only phenol–imine structure is registered at normal conditions. (Dodoff *et al.*, 1999; Percy and Thornton, 1972; Teyssie and Charette, 1963). In our study, ^{1}H-NMR spectra suggests that this is also the case with sulfonylhydrazone derivatives (compounds **4–6**). Because, the signals of the HC=N protons show no splitting, and the position of the signals of the ring protons is typical for aromatic, rather then for quinoid proton. The assignment of the NH signals of compounds **1–6** and OH signals of compounds **4–6** was confirmed by deutero-exchange. It was reported that NH and OH signals of several methane sulfonamide derivatives were observed in the range of 9.40–11.10 and 11.00–11.68 ppm, respectively. Shifting was explained by the existence of intramolecular hydrogen bond between the hydroxyl group and the imine nitrogen atom by the authors (Dodoff *et al.*, 1999).

In compound **1** and **2**, $NH_{(ring)}$ protons are observed at 12.99 and 12.97 ppm; NH protons belong to sulfonic acid hydrazide at 10.01 and 11.22 ppm; azomethine (HC=N) protons at 8.36 and 8.08 ppm (H-10); indole ring protons at 7.94 and 7.62 ppm (H-2), 7.79 and 7.49 ppm (H-5), 7.24 and 7.23 ppm (H-8), 7.08 and 6.96 ppm (H-7), 7.06 and 6.94 ppm (H-6); CH_3 and CH_2 protons bonded to SO_2 at 3.08 and 3.13 ppm (H-11); CH_3 protons bonded to SO_2CH_2 for compound **2** at 1.13 ppm (H-12) (Asiri, 2000; Özbek *et al.*, 2007). ^{1}H NMR spectra of compound **3** exhibit azomethine (HC=N) protons at 8.02 ppm (H-6); thiophene ring protons at 7.47 ppm (H-5), 7.29 ppm (H-3), and 6.97 ppm (H-4) (Balaban *et al.*, 2008); SO_2CH_2 protons at 3.00 ppm (H-7) and CH_3 protons bonded to CH_2 at 1.07 ppm (H-8). In this study, OH and NH signals of compounds **4–6** are observed over 10.00 ppm as singlet at low-field area, and the chemical shift values of OH protons are higher than NH protons. For compound **4** and **5**, OH protons of salicyl ring are observed at 11.35 and 11.71 ppm; NH protons at 10.23 and 10.60 ppm. For compound **6**, OH and NH signals observed at 11.18 and 11.15 ppm are very close to each other. Similar feature has been also observed for hydrazone compounds of 2-hydroxy-1-naphthaldehyde (Dodoff *et al.*, 1999). Azomethine (HC=N) protons for compound **4** and **6** are observed at 8.27 ppm (H-7) and 8.81 (H-11) ppm as singlet. In compound **4** and **5**, aromatic protons are observed at 7.56 and 7.54 ppm (H-6), 7.49 and 7.47 ppm (H-4), 6.92 and 6.92 ppm (H-5), 6.88 and 6.89 ppm (H-3); SO_2CH_2 protons at 3.22 and 3.24 ppm (H-8) and CH_3 protons bonded to CH_2 at 1.22 and 1.27 ppm (H-9); acetyl ($N{=}CCH_3$) protons for compound **5** at 2.32 ppm (H-7a). In compound **6**, naphtyl ring protons are observed at 8.39 ppm (H-10), 7.49 ppm (H-5), 7.43 ppm (H-6), 7.37 ppm (H-8), 7.29 ppm (H-7), and 7.26 ppm (H-3); SO_2CH_2 protons at 3.15 ppm (H-12) and CH_3 protons at 1.15 ppm (H-13).

In ^{13}C NMR spectra, azomethine (CH=N) carbon atoms for compound **1–4**, **6** are observed at 159.6 ppm (C-10), 159.8 ppm (C-10), 142.8 ppm (C-6), 149.7 ppm (C-7) and 138.6 ppm (C-11). Compound **4–6** have the highest chemical shifts at 154.9 ppm, 158.7 ppm and 159.4 ppm (C-2) belong to phenolic carbons. Compound **1** and **2** have the indole carbons which have the highest chemical shifts at 138.7 ppm and 139.6 ppm (C-2) and the lowest chemical shifts at 110.9 ppm and 111.3 ppm (C-8). And also, the other carbons belong to indole ring are observed in these ranges. In compound **3**, the chemical shifts of the thiophene ring are observed at 139.0 ppm (C-2), 131.5 ppm (C-3), 129.5 ppm (C-5) and 128.5 ppm (C-4). CH_3 carbon bonded to SO_2 at 46.7 ppm (C-11) for compound **1**; $SO_2CH_2CH_3$

carbons at 46.9 ppm (C-11) and 9.1 ppm (C-12) for compound **2**; 39.2 ppm (C-7) and 8.6 ppm (C-8) for compound **3**; 45.1 ppm (C-8) and 8.0 ppm (C-9) ppm for compound **4**; 45.6 ppm (C-8) and 8.2 ppm (C-9) for compound **5**; 46.5 ppm (C-12) and 8.6 ppm (C-13) ppm for compound **6**. Acetyl carbon (N=C**C**H_3) of compound **5** is observed at 15.0 ppm (C-7a) ppm.

IR spectra

The assignment of the bands was made taking into consideration the literature data for compounds containing appropriate structural fragments; sulfonamides, sufonylhydrazines, and sulfonylhydrazones, methanesulfonyl derivatives (Dodoff *et al.*, 1999; Percy and Thornton, 1972; Katritzky and Jones, 1960; Bacon *et al.*, 1965). It should be noted the position and shape of the OH-stretching bands in compounds **4–6**. They appear at quite low-wave numbers (2832–2633 cm^{-1}) and are split into several components. Similar feature has been described for a number of Schiff bases derived from salicylaldehyde and has been explained by the participation of the hydroxyl group into hydrogen bond with the imine nitrogen atom (Faniran *et al.*, 1974; Lenco *et al.*, 1999). In the infrared spectra of synthesized compounds, the most characteristic absorptions at 1611–1642 cm^{-1} are assigned to the stretching vibration of the azomethine (–CH=N–) group, the absorptions at 3182–3206 cm^{-1} are assigned to NH groups (Balaban *et al.*, 2003; Hamurcu *et al.*, 2008). Compounds **4–6** also display bands at 1241–1268 cm^{-1} which are assigned to *ν*(C–O) stretching vibrations of the phenolic-*OH*, respectively (Vance *et al.*, 1998). SO_2 group has three vibration types as $\nu_{as}(SO_2)$ observed at 1339–1317 cm^{-1}, $\nu s_{ym}(SO_2)$ at 1160–1142 cm^{-1} and $\delta(SO_2)$ at 537–515 cm^{-1}.

LC–MS spectra

Fragmentation steps of all aromatic/heteroaromatic sulfonylhydrazones in LC–MS spectra are presented in Table 1. Compounds **1–6** give the molecular ions, $[M]^+$ at the desired positions: *m*/*z* (abudance %) = 238.1 (36), 252.0 (33), 217.1 (45), 229.0 (76), 243.0 (100), and 276.9 (17). The fragmentation steps of aromatic/heteroaromatic sulfonylhydrazones are assigned as **fragm**. **I** belong to removal of –SO_2R group, **fragm**. **II** belong to removal of =N–NH–SO_2R, and **fragm**. **III** belong to removal of aromatic/heteroaromatic groups (R″–CR′=) as seen in Table 1 (Özdemir Özmen *et al.*, 2007).

Electrochemical behavior

The electrochemical behavior of aromatic/heteroaromatic sulfonylhydrazones in DMSO at glassy carbon electrode was investigated using cyclic voltammetry (CV), controlled potential electrolysis, and chronoamperometry (CA) techniques. The cyclic voltametry (CV) of compound **1–6** in DMSO containing 0.1 M TBATFB on glassy carbon electrode at a scan rate of 0.01 V s^{-1}(vs. Ag/Ag^+) are exhibited in Figs. 4 and 5. The reduction potentials (E_p^c) of the C=N, OH, and SO_2 groups are presented in Table 2. E_p^c values of the sulfonylhydrazones are evaluated with molecular descriptors for the structure–activity relationship (SAR) analysis.

The number of electrons transferred (*n*) during the reduction of sulfonylhydrazones and their diffusion coefficients (*D*) was determined using ultramicro electrode and chronoamperometry. *n* and *D* values were calculated as follows:

$$n = \frac{n_s S^2 i_s C_s}{S_s^2 iC} \qquad D = \frac{D_s S_s^2 i^2}{S^2 i_s^2}$$

where *i* is limiting steady-state current, *S* is the slope of the of the chronoamperometric *i* vs. $t^{-1/2}$ plot for hydrazone compounds.

The limiting steady-state currents for sulfonylhydrazones were determined using linear sweep voltammetry method. The diffusion coefficient (*D*) is related with the diffused amount of compounds to the electrode surface (Table 3). The heterogeneous standard rate constants (k_s) are found from cyclic voltammogram at different scan rates. In general, as the scan rate is increased, reduction peak potential (E_p^c) and the peak width values ($E_{p/2}$) show a change which affects the value of k_s which is calculated from the formulas below. k_s values at 21 °C, which are independent of *v* (Table 3) and they are the indicator of semireversible behavior (Demirel Özel *et al.*, 2009; Klingler and Kochi 1981).

$$k_s = 2.18\left(\frac{D\beta nFv}{\mathrm{RT}}\right)^{1/2} \qquad \beta = 1.857\frac{\mathrm{RT}}{nF(E_p^c - E_{p/2}^c)}$$

The current function (*i*pc/*v*1/2C) values were plotted against the scan rate (*v*) to apply the Nicholson–Shain criteria. The current function decreases exponentially toward the higher scan rates shows that the mechanism of electron transfer is followed by EC type (Nicholson and Shain 1964), and $2e^-$ transferred reduction occurs in –CH=N– group as shown in Fig. 6. Their action mechanism can be useful for pharmacokinetic and pharmacodynamic purposes in biological systems as drugs.

Antimicrobial activity

The antibacterial screening of the compound was evaluated at the concentration of 400 μg/0.05 mL, and the inhibition zones were measured in mm. The activity results of the sulfonylhydrazones and positive controls (antibiotics and antifungals) are exhibited in Table 4.

Table 1 The fragments of compounds, *m/z* (abudance %)

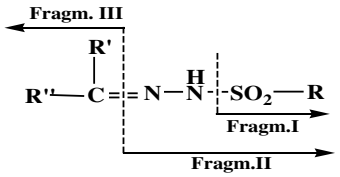

Compound	$[M]^+$ m/z (%)	Fragm. I m/z (%)	Fragm. II m/z (%)	Fragm. III m/z (%)
1	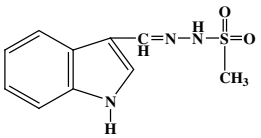 $C_{10}H_{11}N_3SO_2$ 238.1(36)	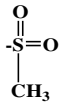 CH_3SO_2 79.2 (23)	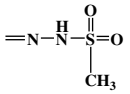 $CH_3N_2SO_2$ 107.1 (87)	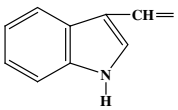 C_9H_7N 128.1(7)
2	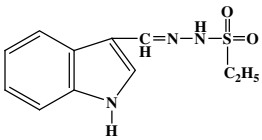 $C_{11}H_{13}N_3SO_2$ 252.0(33)	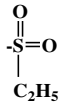 $C_2H_5SO_2$ 93.0 (100)	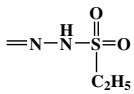 $C_2H_5N_2SO_2$ 121.1 (48)	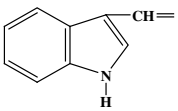 C_9H_7N 128.0(25)
3	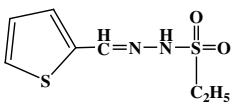 $C_7H_{10}N_2S_2O_2$ 217.1(45)	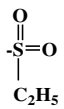 $C_2H_5SO_2$ 91.1 (15)	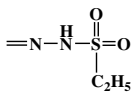 $C_2H_5N_2SO_2$ 122.1 (25)	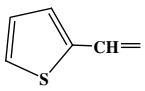 C_5HS 97.0(14)
4	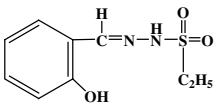 $C_9H_{12}N_2SO_3$ 229.0 (76)	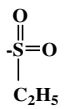 $C_2H_5SO_2$ 93.1 (30)	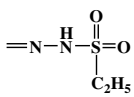 $C_2H_5N_2SO_2$ 121.8 (34)	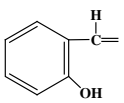 C_7H_6O 106.1(11)
5	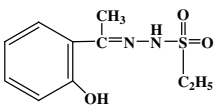 $C_{10}H_{14}N_2SO_3$ 243.0 (100)	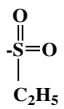 $C_2H_5SO_2$ 93.8 (12)	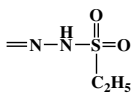 $C_2H_5N_2SO_2$ 121.1 (28)	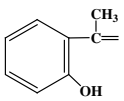 C_8H_8O 121.0(29)
6	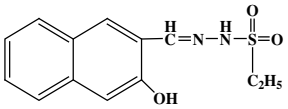 $C_{13}H_{14}N_2SO_3$ 276.9 (17)	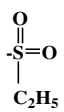 $C_2H_5SO_2$ 93.1 (100)	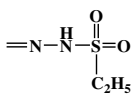 $C_2H_5N_2SO_2$ 121.9 (40)	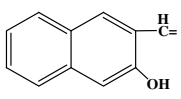 $C_{11}H_8O$ 156.0(45)

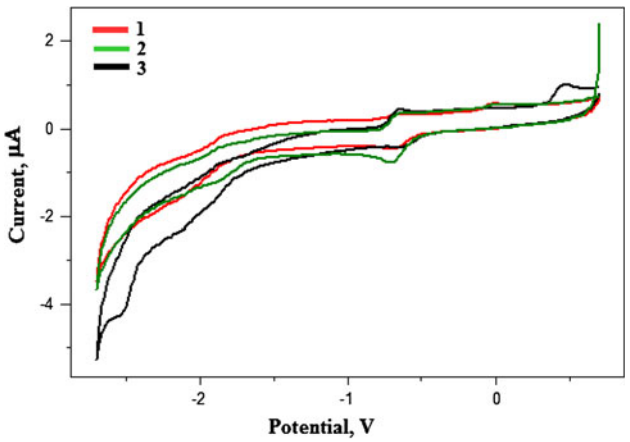

Fig. 4 Cyclic voltammogram (CV) of compound **1–3** in DMSO containing 0.1 M TBATFB on glassy carbon electrode at a scan rate of 0.01 V s^{-1}(vs. Ag/Ag^{+})

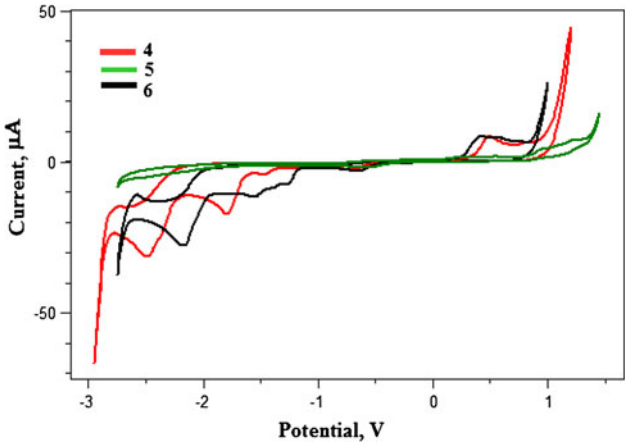

Fig. 5 Cyclic voltammogram (CV) of compound **4–6** in DMSO containing 0.1 M TBATFB on glassy carbon electrode at a scan rate of 0.01 V s^{-1}(vs. Ag/Ag^{+})

The activity results showed that the sulfonylhydrazones have poor activity against microorganism at studied concentration. However, compound **6** has enhanced activity against all microorganism. *Staphylococcus aureus* is the most influenced bacteria against compound **6** having the diameter zones of 27 mm (Fig. 7). Reason of this phenomena can be explained due to presence delocalization of π electrons over the whole aromatic naphtyl ring and also its activity may be arise from the hydroxyl group which may play an important role in the antimicrobial activity. The electronic delocalization supposed within the aromatic ring system may increase the lipophilic character of the compound **6**, and the lipophilicity leads to breakdown of the permeability barrier of the cell and this regards the normal cell processes (Raman *et al.*, 2001). By the way, the entrance of the compounds into the cells increases, and thus, the microorganisms are effected mostly. But, the fungicidal screening including compound **6** shows that ligands have less activity against fungi; *Candida albicans.* Besides, the inhibition zones formed by standard antibiotics (Erythromycin, Vancomycin and Tetracycline) against all bacteria and antifungals (Oxiconazole and Isoconazole) against *Candida albicans* (Keskioğlu *et al.*, 2008; Çete *et al.*, 2006; Katircioglu *et al.* 2006) are reported in Table 4.

Theoretical calculations

The geometry optimization was performed on B3LYP/6-311G(d,p) methods with GAUSSIAN 03 software. And also, the relations between some molecular descriptors and antimicrobial activity, the selected parameters such as logP, dipole moment (DM), surface area (SA), volume (*V*), refractivity (*R*), mass (*M*), hydration enthalpy (ΔH_{hyd}), binding energy (ΔE_b), heat of formation (ΔH_f), and HOMO and LUMO were calculated by Hyperchem 8, PM3-based QSAR models to determine the structure–activity relation (Alyar *et al.*, 2011a, b; Özbek *et al.*, 2009) and tabulated in Table 5.

2-Hydroxy-1-naphth aldehydeethanesulfonylhydrazone (**6**) containing naphtyl group shows higher activity because of the cation–pi interaction and aromatic pi-stacking through the whole ring. The naphthalene having higher electron density may encounter a cation or a positively charged group on protein, receptor site bonds the aromatic ring to make charge-transfer complex. The correlations between molecular descriptors and antimicrobial activities (SAR) show that compound **6** has the highest activity against microorganisms, and its activity is effected with some of the selected desctriptors. These descriptors indicate that the presence of naphtyl ring having big size and especially cation–pi interaction and aromatic pi-stacking through the naphtyl ring may have importance on antimicrobial activity as mentioned by Aslan *et al.*, 2012. And also, electrostatic interactions, electrophilic reactivity control the activity of the compounds. The molecular descriptors suggest that the presence of naphtyl ring plays a dominant role in the microbial activity on as compound **6.**

The octanol–water partition coefficient (log*P*) has been considered as descriptors of the hydrophobic effect. As shown in Table 5, log*P* and size parameters related to surface area, volume, refractivity, and molecular mass increase with a decrease in activity of the compound **6**. The components of the frontier molecular orbitals as well as dipole moment play an important role. The decrease in dipole moment can be used to reasonably explain the rise of the antimicrobial activity in compound **6**. Binding energy is a thermodynamic parameter and refers to the chemical stability of the molecule. In our series, activity increases especially in compound **6** with decreasing binding energy.

Table 2 Reduction peak potentials (E_p^c) of sulfonylhydrazones at different scanning rates

Compound	E_p^c, V (0.01 V s^{-1})	E_p^c, V (0.05 V s^{-1})	E_p^c, V (0.1 V s^{-1})	E_p^c, V (0.5 V s^{-1})	E_p^c, V (1 V s^{-1})	E_p^c, V (5 V s^{-1})
1	−0.69	−0.74	−0.77	−0.83	−0.82	−0.85
2	−0.70	−0.72	−0.75	−0.80	−0.81	−0.93
3	−0.61	−0.74	−0.75	−0.80	−0.81	−0.85
	−2.54	−2.55	−2.57	−2.64	–	–
4	−0.67	−0.73	−0.75	−0.78	−0.83	−0.90
	−1.47	−1.51	−1.52	−1.59	−1.62	−1.69
	−1.80	−1.83	−1.86	−1.95	−1.99	–
	−2.49	−2.57	−2.61	−2.72	−2.84	−2.60
5	−0.57	−0.65	−0.68	−0.75	−0.79	−0.87
	−2.42	−2.45	−2.46	−2.48	−2.51	–
6	−0.64	−0.69	−0.70	−0.77	−0.81	−0.86
	−1.28	−1.29	−1.30	−1.38	−1.42	−1.49
	−1.56	−1.59	−1.64	−1.75	−1.82	−1.91
	−2.18	−2.24	−2.27	−2.39	−2.47	−2.54

Table 3 Electrochemical properties of sulfonylhydrazones

Compound	UME limiting steady-state current (i_{ss}, A)	Cottrell slope (S) of –CH=N– peak	Diffusion coefficients (D, cm^2 $s^{-}1$)	Standard heterogeneous rate constant k_s (cm s^{-1})
1	4.523×10^{-10}	3.124×10^{-5}	2.41×10^{-6}	9.97×10^{-4}
2	2.873×10^{-10}	2.407×10^{-5}	1.64×10^{-6}	9.39×10^{-4}
3	2.331×10^{-10}	2.17×10^{-5}	1.33×10^{-6}	9.12×10^{-4}
4	6.300×10^{-10}	3.86×10^{-5}	3.06×10^{-7}	1.04×10^{-6}
5	5.175×10^{-10}	3.23×10^{-5}	2.95×10^{-7}	1.03×10^{-6}
6	3.634×10^{-10}	2.84×10^{-5}	1.88×10^{-7}	9.59×10^{-7}

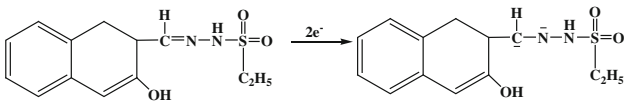

Fig. 6 The reduction mechanism of –CH=N– group in compound **6**

One of the most important descriptors is LUMO energy which describes electrophilicity of the compound, and its level has the importance because of the donor–acceptor interactions. In general, molecules with low-LUMO energy values accept the electrons more easily than the highers. The lower LUMO energy in other words lower LUMO–HOMO energy gap ($\Delta\varepsilon_{LUMO-HOMO}$) affects the noncovalent binding affinities of the compounds to DNA as receptor. The antimicrobial activity of the compound **6** increases with the lowest energy of LUMO and also, $\Delta\varepsilon_{LUMO-HOMO}$ energy gap (Aslan *et al.*, 2012).

Electrochemical study shows that reducing potentials of imine (C=N) group of compound **6** is very close to that of other compounds and has no trendy with activity, but the increasing potentials of OH and SO_2 groups may be explained by the increasing activity of compound **6** (Özbek *et al.*, 2012). In particular, it can be very interesting behavior to explain the SAR's of such similar series, because they have partial differences in their chemical structures, they contrarily have a sharp difference in their activity as seen in compound **6** (Karacan *et al.*, 2012; Özbek *et al.*, 2012). The structure–activity relationships (SAR's) were applied to offer a theoretical reference on the molecular designs of antimicrobial agent (Alyar *et al.*, 2011a, b; Özbek *et al.*, 2012).

Table 4 Antimicrobial activities of compound **1–6** and positive controls as zone diameter (mm)

Compound	*B. cereus* RSKK 863	*S. aureus* ATCC 259231	*M. luteus* NRLL, B-4375	*P. aeroginosa* ATCC 29212	*Y. enterecolitice* ATCC 1501	*C. albicans* ATCC 10239
1	3	>2	>2	4	>2	5
2	3	>2	>2	4	>2	5
3	>2	>2	>2	3	>2	6
4	>2	>2	>2	2	>2	4
5	>2	>2	>2	2	>2	3
6	14	27	13	14	10	3
Erythromycin[a]	23	17	31	>2	>2	–
Vancomycin[a]	12	8	16	>2	>2	–
Tetracycline[a]	17	15	23	4	16	–
Oxiconazole[b]	–	–	–	–	–	17
Isoconazole[b]	–	–	–	–	–	17

[a] Standard antibiotic and [b] standard antifungal ref. (Rohrbaugh and Jurs, 1987; Percy and Thornton, 1972; Teyssie and Charette, 1963)

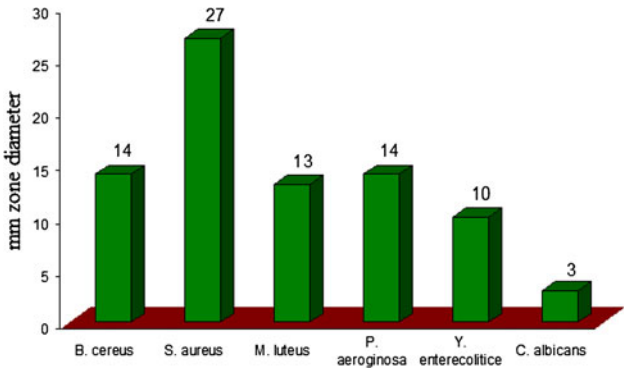

Fig. 7 Antimicrobial activities of compound **6** against bacteria

Table 5 Calculated molecular descriptors for compound **1–6**

Compound	log*P*	DM (D)	SA (Å^2)	V (Å^3)	R (Å^3)	M (amu)	ΔH_{hyd} (kcal mol^{-1})	B.E. (kcal mol^{-1})	ΔH_f (kcal mol^{-1})	HOMO (eV)	LUMO (eV)	$\Delta\varepsilon_{LUMO-HOMO}$ (eV)
1	−1.22	4.87	394.37	675.71	66.22	237.28	−13.12	−2,799.31	7.23	−8.44	−0.61	7.83
2	−0.88	5.28	422.72	733.19	70.97	251.30	−11.79	−2,689.88	−55.57	−9.14	−0.71	8.43
3	−0.44	4.26	393.59	617.27	56.97	218.29	−9.34	−2,197.86	−2.69	−9.23	−0.95	8.28
4	−0.07	5.28	403.12	661.25	61.28	228.27	−12.68	−2,689.88	−55.57	−9.14	−0.71	8.43
5	−0.07	5.05	403.12	661.25	61.28	228.27	−12.68	−2,970.22	−60.82	−9.33	−0.55	8.78
6	0.00	3.68	427.17	780.92	79.48	278.33	−13.03	−3,463.81	−41.73	−8.64	−0.97	7.68

Conclusions

The molecular structure of the aromatic/heteroaromatic sulfonylhydrazones was discussed in this article on the basis of spectroscopic methods (^{1}H and ^{13}C NMR, FT-IR, LC–MS) and optimized by DFT calculations carried out using Becke's three-parameter hybrid functional (B3LYP) method. The electrochemical behaviors of aromatic/heteroaromatic sulfonylhydrazones were evaluated by means of cyclic voltammetry (CV), controlled potential electrolysis, and chronoamperometry (CA) techniques. Electrochemical reduction mechanism of compound **1–6** was also proposed that sulfonylhydrazones follow EC mechanism which follows semireversible electron transfer steps.

Antibacterial activity and the structural relationships (SAR's) of the compounds showed that activity of the compound **6** increases weakly to the increasing log*P* values, surface area (SA), volume (*V*), refractivity (*R*), and molecular mass and reduction potential of OH, SO_2 groups. The reduction potential of C=N group, hydration enthalpy (ΔH_{hyd}), heat of formation (ΔH_f), HOMO energy values can not be correlated with the activity while dipole moment (DM), binding energy (ΔE_b), LUMO–HOMO energy gap decrease with the increasing activity.

Acknowledgments This research was supported by Gazi University Research Found under Project No. 05/03-15. The authors thank TUBİTAK for allocation of time at the ^{1}H–^{13}C-NMR, LCMS, and elemental analyses.

References

Aleksic M, Kapetanovic V, Zuman P (2004) Polarographic and Voltammetric Behavior of the Antibiotic Cefetamet; reduction of the Methoxyimino group. Collect Czech Chem Commun 69:1429–1442

Alyar S, Karacan N (2009) Synthesis, characterization, antimicrobial activity and structure–activity relationships of new aryldisulfonamides. J Enzyme Inhib Med Chem 24:986–992

Alyar S, Karacan N, Özbek N, Kuzukıran K (2011a) Quantitative structure–activity relationships studies for prediction of antimicrobial activity of synthesized disulfonamide derivatives. Med Chem Res 20:175–183

Alyar S, Zengin H, Özbek N, Karacan N (2011b) Synthesis, characterization, spectroscopic properties, theoretical calculation and antimicrobial activity of new aryldisulfonamides. J Mol Struct 992:27–32

Alyar H, Alyar S, Ünal A, Özbek N, Şahin E, Karacan N (2012a) Synthesis, characterization and antimicrobial activity of m-toluenesulfonamide, *N*,*N*′-1,2-ethanediylbis (mtsen) and [Cu(II)(phenanthroline)2]mtsen complex. J Mol Struct 1028:116–125

Alyar H, Ünal A, Ozbek N, Aylar S, Karacan N (2012b) Conformational analysis, vibrational and NMR spectroscopic study of the methanesulfonamide-*N*,*N*'-1,2-ethanediylbis. Spectrochim Acta A 91:39–47

Asiri AM (2000) (Indol-3-yl)barbituric acid. Molecules 5:M183

Aslan HG, Özcan S, Karacan N (2012) The antibacterial activity of some sulfonamides and sulfonyl hydrazones, and 2D-QSAR study of a series of sulfonylhydrazones. Spectrochim Acta A 98:329–336

Bacon N, Boulton AJ, Brownlee RTC, Katritzky AR, Topsom RD (1965) Infrared absorption of substituents in heterocyclic systems. Amine–imine tautomerism by infrared spectroscopy. J Chem Soc Part IX:5230–5233

Bajaj S, Sambi SS, Madan AK (2005) Prediction of anti-inflammatory activity of *N*-arylanthranilic acids: computational approach using refined Zagreb indices. Croat Chem Acta 78:165–174

Balaban A, Sekerci M, Erk B (2003) Synthesis, physico-chemical characterization, and stability constants of metal complexes of pyridine-2-carbaldehyde thiosemicarbazone. Synth React Inorg Met-Org Chem 33:1775–1786

Balaban A, Çolak N, Ünver H, Erk B, Durlu TN, Zengin DM (2008) Synthesis, spectroscopic studies and crystal structure of *N*,*N*′-bis((thiophene-2-carboxamido)propyl)piperazine. J Chem Cryst 38:369–372

Baymak MS, Celik H, Lund H, Zuman P (2003) Contribution to electroreduction of hydrazones. Electrochem Soc 12:94–96

Çete S, Dişli A, Yıldırır Y, Yaşar A (2006) Synthesis and antimicrobial effects of some phenylazopropanedinitriles and their derivatives. Asian J Chem 18:2061–2066

de Souza MVN (2005) Synthesis and biological activity of natural thiazoles: an important class of heterocyclic compounds. J Sulfur Chem 26:429–449

Demirel Özel A, Durmuş Z, Çukurovalı A, Yılmaz İ, Kılıç E (2009) Electroreduction of some substituted hydrazones on platinum electrode in dimethylformamide. Acta Chim Slovencia 56:797–806

Dodoff NI, Özdemir Ü, Karacan N, Gorgieva M, Konstantinov SM, Stefanova ME (1999) Schiff bases of methanesulfonylhydrazine. Synthesis, spectroscopic characterization, conformational analysis and biological activity. Z Naturforsch 54:1553–1562

Faniran JA, Patel KS, Bailar JC (1974) Infrared spectra of *N*,*N*′-bis(salicylidene)-1,1-(dimethyl)ethylenediamine and its metal complexes. J Inorg Nucl Chem 36:1547–1551

Finlay GJ, Baguley BC, Snow K, Judd W (1990) Multiple patterns of resistance of human leukemia cell sublines to amsacrine analogues. Natl Cancer Inst 82:662–667

Hamurcu F, Balaban Gündüzalp A, Çete S, Erk B (2008) The synthesis, characterization and antimicrobial activity of *N*,*N*′-bis(2-thiophenecarboxamido)-1,3-diaminopropane and *N*,*N*′-bis(2-furancarboxamido)-1,3-diaminopropane and their Cu(II), Zn(II), Co(III) complexes. Trans Met Chem 33:137–141

Jensen PB, Sorensen BS, Demant EJ, Sehested M, Jensen PS, Vindelov L, Hansen HH (1990) Antagonistic effect of aclarubicin on the cytotoxicity of etoposide and 4′-(9-acridinylamino)methanesulfon-*m*-anisidide in human small cell lung cancer cell lines and on topoisomerase II-mediated DNA cleavage. Cancer Res 50:3311–3316

Karacan MS, Yakan Ç, Yakan M, Karacan N, Zharmukhamedov SK, Shitov A, Los DA, Klimov VV, Allakhverdiev SI (2012) Quantitative structure–activity relationship analysis of perfluoroisopropyldinitrobenzene derivatives known as photosystem II electron transfer inhibitors. Biochim Biophys Acta 1817:1229–1237

Katircioglu H, Beyatlı Y, Aslim B, Yuksekdağ Z, Atici Z (2006) Screening for antimicrobial agent production of some microalgae in freshwater. Internet J Microbiol 2(2):1–9

Katritzky AR, Jones RA (1960) Infrared absorption of substituents in aromatic systems. Part VI. Methanesulphonamides. J Chem Soc 4497–4499

Keskioğlu E, Balaban Gündüzalp A, Çete S, Hamurcu F, Erk B (2008) Cr(III), Fe(III) and Co(III) complexes of tetradentate (ONNO) Schiff base ligands: synthesis, characterization, properties and biological activity. Spectrochim Acta A 70:8634–8640

Klingler RJ, Kochi JK (1981) Electron-transfer kinetics from cyclic voltammetry. Quantitative description of electrochemical reversibility. J Phys Chem 85:1731–1741

Lenco A, Mealli C, Paoli P, Dodoff N, Kantarcı Z, Karacan N (1999) Structure and vibrational spectroscopy of methanesulfonic acid hydrazide: an experimental and theoretical study. New J Chem 23:1253–1256

Nicholson RS, Shain I (1964) Theory of stationary electrode polarography: single scan and cyclic methods applied to reversible, irreversible and kinetic systems. Anal Chem 36:706–723

Özbek N, Katırcıoğlu H, Karacan N, Baykal T (2007) Synthesis, characterization and antimicrobial activity of new aliphatic sulfonamide. Bioorg Med Chem 15:5105–5109

Özbek N, Aylar S, Karacan N (2009) Experimental and theoretical studies on methanesulfonic acid 1-methylhydrazide: antimicrobial activities of its sulfonyl hydrazone derivatives. J Mol Struct 938:48–53

Özbek N, Aylar S, Mamaş S, Şahin E, Karacan N (2012) Synthesis, crystal structure, antibacterial activities, and electrochemical

studies of new *N*,*N*′-polymethylene bis-sulfonamides. J Mol Struct 1010:1–7

Özçelik S, Dinçer M, Şekerci M, Balaban A, Özdemir Ü (2004) *N*-Phenyl-*N*-(2-thienylmethylene)hydrazine. Acta Crystallogr Sect E 60:1552–1553

Özdemir Özmen Ü, Olgun G (2008) Synthesis, characterization and antibacterial activity of new sulfonyl hydrazone derivatives and their nickel(II) complexes. Spectrochim Acta A 70:641–645

Özdemir Ü, Sentürk OS, Sert S, Karacan N, Ugur F (2003) Photochemical reactions of metal carbonyls [M(CO)6 (M Cr, Mo, W), Re(CO)5Br, Mn(CO)3Cp] with 2-hydroxyacetophenone methanesulfonylhydrazone (apmsh). Trans Met Chem 28:443–446

Özdemir Ü, Karacan N, Şentürk OS, Sert S, Uğur F (2004) Synthesis and characterization of metal carbonyl complexes of M(CO)(6)(M Cr, Mo, and W), Re(CO)(5)Br, and Mn(CO)(3)CP with-acetone methanesulfonylhydrazone (amsh) and methanesulfonylhydrazone (msh). Synth React Inorg Met-Org Chem 34:1057–1067

Özdemir Ü, Şentürk OS, Sert S, Karacan N, Uğur F (2006) Reaction of metal carbonyls with 2-hydroxy-1-napthaldehyde methanesulfonylhydrazone and characterization of the substitution products. J Coord Chem 59:1905–1911

Özdemir Ü, Güvenç P, Şahin E, Hamurcu F (2009) Synthesis, characterization and antibacterial activity of new sulfonamide derivatives and their nickel(II), cobalt(II) complexes. Inorg Chim Acta 362:2613–2618

Özdemir Ü, Arslan F, Hamurcu F (2010) Synthesis, characterization, antibacterial activities and carbonic anhydrase enzyme inhibitor effects of new arylsulfonylhydrazone and their Ni(II), Co(II) complexes. Spectrochim Acta A 75:121–126

Özdemir ÖÜ, Akkaya N, Özbek N (2013) New Ni(II), Pd(II), Pt(II) complexes with aromatic methanesulfonylhydrazone based ligands. Synthesis, spectroscopic characterization and in vitro antibacterial evaluation. Inorg Chim Acta 400:13–19

Percy GC, Thornton DA (1972) N-aryl salicylaldimine complexes: ınfrared and PMR spectra of the ligands and vibrational frequencies of their metal(II) chelates. Inorg Nucl Chem 34:3357–3367

Raman N, Kulandaisamy A, Shunmugasundaram A, Jeyasubramanian K (2001) Synthesis, spectral, redox and antimicrobial activities of Schiff base complexes derived from 1-phenyl-2,3-dimethyl-4-aminopyrazol-5-one and acetoacetanilide. Trans Met Chem 26:131–135

Rohrbaugh RH, Jurs PC (1987) Description of molecular shape applied in studies of structure/activity and structure/property relationships. Anal Chim Acta 199:99–109

Sert S, Senturk OS, Ozdemir U, Karacan N, Ugur F (2004) Synthesis and characterization of the products reaction of metal carbonyls[M(CO)6 (M Cr, Mo, W), Re (CO)5Br, Mn(CO)3Cp] with salicylaldehyde methanesulfonyl-hydrazone. J Coord Chem 57:183–188

Teyssie P, Charette JJ (1963) Physico-chemical properties of co-ordinating compounds-III: infra-red spectra of *N*-salicyclidenealkyl-amines and their chelates. Spectrochim Acta A 19:1407–1423

Vance AL, Alcock NW, Heppert JA, Busch DH (1998) An octahedral template based on a new molecular turn: synthesis and structure of a model complex and a reactive, diphenolic ligand and its metal complexes. Inorg Chem 37:6912–6920